Sound transmission prediction by 3-D elasticity theory

Changzheng[1,*], Steven R. Nutt[1]

1. Department of Chemical Engineering and Materials Science, University of Southern California, 3651 Watt Way, VHE 602, Los Angeles, CA 90089-0241, United States

Abstract: The problem of sound transmission through layered panel structures is studied with the exact theory of three-dimensional (3-D) elasticity. The exact solution to the 3-D elasticity equations is obtained by the use of the Fourier spectral method. Based on this analytical solution, a transfer matrix is derived that relates the spectral displacements and stresses on the one surface of the panel to those on the opposite panel surface. The transfer matrix is then used to develop the analytical solutions for sound reflection and transmission coefficients. Explicit, concise expressions are obtained for the analytical solutions of the acoustic transmission and reflection coefficients under the general conditions of layered anisotropic panels. Examples are given for both single-layer and sandwich panels. Predictions on sound transmission from the 3-D elasticity theory are compared with available data from other methods, and the results are discussed.

Key words: Sound transmission; Elasticity theory; Analytical method; Sandwich panel

*Corresponding author: Tel.: +1 213 740 8929; fax: +1 213 740 7797. E-mail: changzh@usc.edu

1. Introduction

Sound transmission through panel structures is a practical engineering problem that has been studied extensively. Multi-layer panels, particularly three-layer sandwich panels comprised of a thick lightweight core between two face sheets, are commonly used as wall partitions, airplane flooring, and cabin structures. For these applications, panels are designed to minimize the transmission of

Please cite this article as: Changzheng Huang, Steven Nutt, **Sound transmission prediction by 3-D elasticity theory**, Applied Acoustics, Volume 70, Issue 5, May 2009, Pages 730-736, ISSN 0003-682X, http://dx.doi.org/10.1016/j.apacoust.2008.09.003.

noise from external sources. The work by Kurtze and Watters [1] is a classic example of early efforts in designing panels with high transmission loss or high damping.

The methodology for the study of sound transmission through panels can be classified according to the use of experimental [2], numerical [3], or analytical [4-16] approaches. In the analytical approach, the Fourier spectral method, also known as the modal expansion method, is often used to obtain an analytical solution to the governing equations. The most general governing equations for the panel vibration problem are the full 3-D elasticity equations. Under certain conditions, these equations can be reduced to simpler governing equations such as the bending wave equation. Prior analytical studies have largely focused on using reduced governing equations of some kind to obtain a solution for the sound transmission problem. Using this solving strategy, researchers have studied the sound transmission characteristics through various sandwich panels [4], [5], [6], [7], [8] and [9]. In addition, Sewell [10] investigated transmission of diffuse sound through a single-leaf partition, while some other researchers [11] considered sound transmission through double-leaf partitions. Guyader and Lesueur [12] studied acoustic transmission through orthotropic multi-layered plates.

In general, the predictions of sound transmission from reduced equations are accurate for certain specific types of panels, such as a thin panel. For more general anisotropic panels, however, the validity of these reduced governing equations is difficult to justify. With the increased use of laminated composites that are generally anisotropic in nature [3] and [13], reliable analysis requires more accurate governing equations or the full 3-D elasticity equations. Munjal [14] derived transfer matrices for multi-layered plates with each layer assumed to be isotropic. Others used a 3-D model to study sound transmission across orthotropic laminates by neglecting either one or two shear waves [15] and [16]. Additional studies that have employed the 3-D model to study laminated composites include the work done by the group of Liu [17], [18] and [19], by Skelton and James [20], and by

Please cite this article as: Changzheng Huang, Steven Nutt, **Sound transmission prediction by 3-D elasticity theory**, Applied Acoustics, Volume 70, Issue 5, May 2009, Pages 730-736, ISSN 0003-682X, http://dx.doi.org/10.1016/j.apacoust.2008.09.003.

Ye [21]. In the approach of Liu [17], [18] and [19], the 3-D elasticity equation is reduced to a sixth-order ordinary differential equation for each layer. In other words, there are six unknowns to be determined in each layer. In this approach, for an *N*-layer laminate, a system of 6*N* linear equations must be solved. In contrast, Skelton and James [20] used the transfer matrix method. The transfer matrix method was also adopted by Ye [21], but under a different name the state space method. In the transfer matrix approach, a reduced system of only six linear equations must be solved, regardless of the number of laminate layers. This simplifies the analysis, and results in computational savings. Although the 3-D models described above are general and may be applicable to anisotropic layered structures, no explicit analytical solutions have been reported in these studies for the acoustic transmission and reflection coefficients under general conditions. The purpose of the present study is to show that an exact and explicit analytical solution can indeed be derived for the acoustic transmission and reflection coefficients for the general cases of multi-layered anisotropic panels. We achieve this by adopting the rigorous approach of the transfer matrix method. In addition to providing physical insights into the structure-wave interaction, the concise and explicit expressions of the analytical solution also provide a quick way of making predictions for sound transmission through multi-layer planar panels. In the following section, we develop formulations for solving the 3-D elasticity equations and for obtaining the sound transmission coefficient. This is followed by a presentation of examples and numerical results that include predictions of sound transmission by the exact 3-D elasticity theory.

Please cite this article as: Changzheng Huang, Steven Nutt, **Sound transmission prediction by 3-D elasticity theory**, Applied Acoustics, Volume 70, Issue 5, May 2009, Pages 730-736, ISSN 0003-682X, http://dx.doi.org/10.1016/j.apacoust.2008.09.003.

2. Theory

A schematic diagram for sound transmission analysis is shown in Fig. 1. A structural panel of thickness *h* separates two infinite regions of ambient fluid medium. In this study, we consider the ambient fluid to be air. As a plane sound wave is incident on the bottom surface of the panel, part of the acoustic energy will be reflected back into the lower region, part of the energy will be absorbed by the panel due to material damping, and the remainder will transmit through the panel and be radiated into the upper region. The acoustic transmission efficiency is the primary focus of the present study.

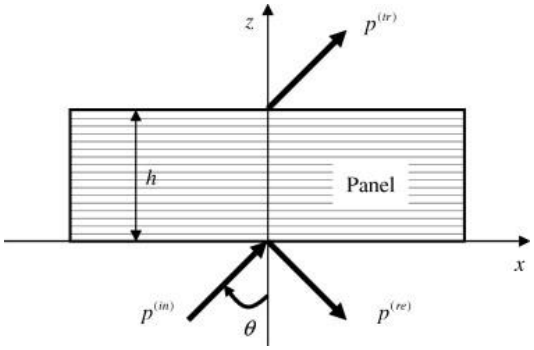

Fig. 1. *A schematic diagram of a sound wave $p^{(in)}$ incident on a panel of thickness h from the bottom surface with an incident angle θ. The reflected and transmitted waves are denoted as $p^{(re)}$ and $p^{(tr)}$, respectively. The incident wave lies in the xz-plane, which makes the azimuthal angle $\phi = 0$.*

The sound energy radiated from the panel depends on the dynamic movement of the panel surfaces in contact with the ambient air. The movements of the two panel surfaces are also related. In the Fourier spectral domain, this relationship is manifest by a transfer matrix that relates the spectral displacements and stresses on one surface to those on the other surface. In the following section, the general transfer matrix based on the 3-D elasticity equations is derived, followed by the derivation of sound transmission coefficient. We employ matrix notations for convenience and compactness.

Please cite this article as: Changzheng Huang, Steven Nutt, **Sound transmission prediction by 3-D elasticity theory**, Applied Acoustics, Volume 70, Issue 5, May 2009, Pages 730-736, ISSN 0003-682X, http://dx.doi.org/10.1016/j.apacoust.2008.09.003.

2.1 3-D elasticity equations

Consider the vibration of a single-layer panel as depicted in Fig. 1. The panel dynamics is governed by the 3-D elasticity equations

$$\begin{aligned}
\frac{\partial \sigma_{xx}}{\partial x}+\frac{\partial \sigma_{yx}}{\partial y}+\frac{\partial \sigma_{zx}}{\partial z}&=\rho\frac{\partial^2 u}{\partial t^2}\\
\frac{\partial \sigma_{xy}}{\partial x}+\frac{\partial \sigma_{yy}}{\partial y}+\frac{\partial \sigma_{zy}}{\partial z}&=\rho\frac{\partial^2 v}{\partial t^2}\\
\frac{\partial \sigma_{xz}}{\partial x}+\frac{\partial \sigma_{yz}}{\partial y}+\frac{\partial \sigma_{zz}}{\partial z}&=\rho\frac{\partial^2 w}{\partial t^2}.
\end{aligned} \tag{1}$$

Here ρ is the density of the panel, and

$$\begin{aligned}
\mathbf{u}&=(u,v,w)^{\mathrm{T}}\\
\boldsymbol{\sigma}&=(\sigma_{xx},\sigma_{yy},\sigma_{zz},\sigma_{yz},\sigma_{zx},\sigma_{xy})^{\mathrm{T}}
\end{aligned} \tag{2}$$

are column vectors of displacements and stresses, respectively. With tensor notation, Eq. (1) can be written as

$$\mathbf{D}\boldsymbol{\sigma}=\rho\frac{\partial^2 \mathbf{u}}{\partial t^2}. \tag{3}$$

Here **D** is a differential operator defined as

$$\begin{aligned}
\mathbf{D}=\mathbf{D}_1\frac{\partial}{\partial x}+\mathbf{D}_2\frac{\partial}{\partial y}+\mathbf{D}_3\frac{\partial}{\partial z}&=\begin{pmatrix}1&0&0&0&0&0\\0&0&0&0&0&1\\0&0&0&0&1&0\end{pmatrix}\frac{\partial}{\partial x}\\
&+\begin{pmatrix}0&0&0&0&0&1\\0&1&0&0&0&0\\0&0&0&1&0&0\end{pmatrix}\frac{\partial}{\partial y}+\begin{pmatrix}0&0&0&0&1&0\\0&0&0&1&0&0\\0&0&1&0&0&0\end{pmatrix}\frac{\partial}{\partial z}
\end{aligned} \tag{4}$$

It the equation above, we have defined three Boolean matrices $\mathbf{D}_1$, $\mathbf{D}_2$, and $\mathbf{D}_3$. To make it general, we consider an anisotropic stress–strain relationship

$$\begin{pmatrix} \sigma_{xx} \\ \sigma_{yy} \\ \sigma_{zz} \\ \sigma_{yz} \\ \sigma_{zx} \\ \sigma_{xy} \end{pmatrix} = \begin{pmatrix} C_{11} & C_{12} & C_{13} & C_{14} & C_{15} & C_{16} \\ C_{21} & C_{22} & C_{23} & C_{24} & C_{25} & C_{26} \\ C_{31} & C_{32} & C_{33} & C_{34} & C_{35} & C_{36} \\ C_{41} & C_{42} & C_{43} & C_{44} & C_{45} & C_{46} \\ C_{51} & C_{52} & C_{53} & C_{54} & C_{55} & C_{56} \\ C_{61} & C_{62} & C_{63} & C_{64} & C_{65} & C_{66} \end{pmatrix} \begin{pmatrix} \partial u/\partial x \\ \partial v/\partial y \\ \partial w/\partial z \\ \partial w/\partial y + \partial v/\partial z \\ \partial u/\partial z + \partial w/\partial x \\ \partial v/\partial x + \partial u/\partial y \end{pmatrix}. \tag{5}$$

In tensor notation, Eq. (5) can be written as

$$\boldsymbol{\sigma}=\mathbf{C}\mathbf{D}^{\mathrm{T}}\mathbf{u}. \tag{6}$$

Combining Eqs. (3) and (6) yields

$$\mathbf{D}\mathbf{C}\mathbf{D}^{T}\mathbf{u} = \rho\frac{\partial^2\mathbf{u}}{\partial t^2}. \tag{7}$$

2.2 Time harmonic solution

We consider the time harmonic solution

$$\begin{aligned} \mathbf{u}(x,y,z,t) &= \hat{\mathbf{u}}(z)\mathrm{e}^{\mathrm{i}k_x x}\mathrm{e}^{\mathrm{i}k_y y}\mathrm{e}^{-\mathrm{i}\omega t} \\ \boldsymbol{\sigma}(x,y,z,t) &= \hat{\boldsymbol{\sigma}}(z)\mathrm{e}^{\mathrm{i}k_x x}\mathrm{e}^{\mathrm{i}k_y y}\mathrm{e}^{-\mathrm{i}\omega t}. \end{aligned} \tag{8}$$

Here, ω is the circular frequency, and *kx* and *ky* are two in-plane wave numbers. For incident wave induced panel vibration, these two in-plane wave numbers are determined by the contact continuity at the panel-fluid interface. Substitution of Eq. (8)into Eq. (7) yields

$$\mathbf{B}_2 \frac{\mathrm{d}}{\mathrm{d}z}\left(\frac{\mathrm{d}\hat{\mathbf{u}}}{\mathrm{d}z}\right) + \mathbf{B}_1 \frac{\mathrm{d}\hat{\mathbf{u}}}{\mathrm{d}z} + \mathbf{B}_0 \hat{\mathbf{u}} = -\rho\omega^2 \hat{\mathbf{u}}, \tag{9}$$

where the matrices $\mathbf{B}_2$, $\mathbf{B}_1$, and $\mathbf{B}_0$ are given by

$$\begin{aligned}
\mathbf{B}_2 &= \mathbf{D}_3 \mathbf{C} \mathbf{D}_3^{\mathrm{T}} \\
\mathbf{B}_1 &= (\mathrm{i}k_x)\mathbf{D}_1 \mathbf{C} \mathbf{D}_3^{\mathrm{T}} + (\mathrm{i}k_x)\mathbf{D}_3 \mathbf{C} \mathbf{D}_1^{T} + (\mathrm{i}k_y)\mathbf{D}_2 \mathbf{C} \mathbf{D}_3^{\mathrm{T}} + (\mathrm{i}k_y)\mathbf{D}_3 \mathbf{C} \mathbf{D}_2^{\mathrm{T}} \\
\mathbf{B}_0 &= (\mathrm{i}k_x)(\mathrm{i}k_x)\mathbf{D}_1 \mathbf{C} \mathbf{D}_1^{\mathrm{T}} + (\mathrm{i}k_y)(\mathrm{i}k_y)\mathbf{D}_2 \mathbf{C} \mathbf{D}_2^{\mathrm{T}} + (\mathrm{i}k_x)(\mathrm{i}k_y)\mathbf{D}_1 \mathbf{C} \mathbf{D}_2^{\mathrm{T}} \\
&\quad + (\mathrm{i}k_y)(\mathrm{i}k_x)\mathbf{D}_2 \mathbf{C} \mathbf{D}_1^{\mathrm{T}}.
\end{aligned} \tag{10}$$

Eq. (9) is a second-order ordinary differential equation, and it can be cast into a first-order ordinary differential equation by introducing a new variable

$$\hat{\boldsymbol{\xi}} = \frac{\mathrm{d}\hat{\mathbf{u}}}{\mathrm{d}z}. \tag{11}$$

Combining Eqs. (9) and (11) gives rise to

$$\frac{\mathrm{d}}{\mathrm{d}z}\begin{pmatrix}\hat{\mathbf{u}} \\ \hat{\boldsymbol{\xi}}\end{pmatrix} = \begin{pmatrix} \mathbf{I}_0 & \mathbf{I}_1 \\ \left[-\rho\omega^2 \mathbf{B}_2^{-1} - \mathbf{B}_2^{-1}\mathbf{B}_0\right] & \left[-\mathbf{B}_2^{-1}\mathbf{B}_1\right] \end{pmatrix}\begin{pmatrix}\hat{\mathbf{u}} \\ \hat{\boldsymbol{\xi}}\end{pmatrix} = \mathbf{A}\begin{pmatrix}\hat{\mathbf{u}} \\ \hat{\boldsymbol{\xi}}\end{pmatrix}. \tag{12}$$

Here $\mathbf{I}_0$ and $\mathbf{I}_1$ are 3×3 matrices,

$$\mathbf{I}_0 = \begin{pmatrix} 0 & 0 & 0 \\ 0 & 0 & 0 \\ 0 & 0 & 0 \end{pmatrix}, \quad \mathbf{I}_1 = \begin{pmatrix} 1 & 0 & 0 \\ 0 & 1 & 0 \\ 0 & 0 & 1 \end{pmatrix}. \tag{13}$$

The solution for Eq. (12) is

$$\begin{pmatrix}\hat{\mathbf{u}}(z) \\ \hat{\boldsymbol{\xi}}(z)\end{pmatrix} = \mathrm{e}^{\mathbf{A}z}\begin{pmatrix}\hat{\mathbf{u}}(0) \\ \hat{\boldsymbol{\xi}}(0)\end{pmatrix}. \tag{14}$$

Eq. (12) can be used with Eq. (6) to obtain the solution for the stresses

$$\begin{aligned}\hat{\boldsymbol{\sigma}}(z) &= \left(\left[\mathrm{i}k_x \mathbf{C}\mathbf{D}_1^{\mathrm{T}} + \mathrm{i}k_y \mathbf{C}\mathbf{D}_2^{\mathrm{T}} \right] \quad \left[\mathbf{C}\mathbf{D}_3^{\mathrm{T}} \right] \right) \begin{pmatrix} \hat{\mathbf{u}}(z) \\ \hat{\boldsymbol{\xi}}(z) \end{pmatrix} \\ &= \mathbf{H} \begin{pmatrix} \hat{\mathbf{u}}(z) \\ \hat{\boldsymbol{\xi}}(z) \end{pmatrix} = \mathbf{H} \mathrm{e}^{\boldsymbol{\Lambda} z} \begin{pmatrix} \hat{\mathbf{u}}(0) \\ \hat{\boldsymbol{\xi}}(0) \end{pmatrix}. \end{aligned} \tag{15}$$

The stress vector can be re-arranged into two sub-vectors. The first sub-vector consists of the three z-component stresses, while the remaining stresses constitute the second sub-vector, i.e. ,

$$\hat{\boldsymbol{\sigma}} = \begin{pmatrix} \sigma_{xx} \\ \sigma_{yy} \\ \sigma_{zz} \\ \sigma_{yz} \\ \sigma_{zx} \\ \sigma_{xy} \end{pmatrix} = \begin{pmatrix} 0 & 0 & 0 & 1 & 0 & 0 \\ 0 & 0 & 0 & 0 & 1 & 0 \\ 0 & 0 & 1 & 0 & 0 & 0 \\ 0 & 1 & 0 & 0 & 0 & 0 \\ 1 & 0 & 0 & 0 & 0 & 0 \\ 0 & 0 & 0 & 0 & 0 & 1 \end{pmatrix} \left(\begin{pmatrix} \sigma_{zx} \\ \sigma_{yz} \\ \sigma_{zz} \end{pmatrix} \right) = \mathbf{G} \begin{pmatrix} \hat{\boldsymbol{\sigma}}' \\ \hat{\boldsymbol{\sigma}}'' \end{pmatrix}. \tag{16}$$

Then Eq. (15) becomes

$$\mathbf{G} \begin{pmatrix} \hat{\boldsymbol{\sigma}}'(z) \\ \hat{\boldsymbol{\sigma}}''(z) \end{pmatrix} = \mathbf{H} \mathrm{e}^{\boldsymbol{\Lambda} z} \begin{pmatrix} \hat{\mathbf{u}}(0) \\ \hat{\boldsymbol{\xi}}(0) \end{pmatrix}. \tag{17}$$

Eqs. (14) and (17) provide the solution for the spectral displacements and stresses.

2.3 Transfer matrix

We now derive the transfer matrix that relates the spectral displacements and stresses on the top surface $z = h$ with those on the bottom surface $z = 0$. Setting $z = h$ in Eqs.(14) and (17) leads to

$$\begin{pmatrix} \hat{\mathbf{u}}(h) \\ \hat{\boldsymbol{\xi}}(h) \end{pmatrix} = \mathrm{e}^{\boldsymbol{\Lambda} h} \begin{pmatrix} \hat{\mathbf{u}}(0) \\ \hat{\boldsymbol{\xi}}(0) \end{pmatrix} = \mathbf{J} \begin{pmatrix} \hat{\mathbf{u}}(0) \\ \hat{\boldsymbol{\xi}}(0) \end{pmatrix}, \tag{18}$$

$$\begin{pmatrix} \hat{\boldsymbol{\sigma}}'(h) \\ \hat{\boldsymbol{\sigma}}''(h) \end{pmatrix} = \mathbf{G}^{-1}\mathbf{H}e^{\mathbf{A}h}\begin{pmatrix} \hat{\mathbf{u}}(0) \\ \hat{\boldsymbol{\xi}}(0) \end{pmatrix} = \mathbf{K}\begin{pmatrix} \hat{\mathbf{u}}(0) \\ \hat{\boldsymbol{\xi}}(0) \end{pmatrix}. \tag{19}$$

Setting $z = 0$ in Eq. (17) yields

$$\mathbf{G}\begin{pmatrix} \hat{\boldsymbol{\sigma}}'(0) \\ \hat{\boldsymbol{\sigma}}''(0) \end{pmatrix} = \mathbf{H}\begin{pmatrix} \hat{\mathbf{u}}(0) \\ \hat{\boldsymbol{\xi}}(0) \end{pmatrix}. \tag{20}$$

The variables in Eqs. (18), (19) and (20) can be re-arranged. A suitable variable transformation is introduced in Eqs. (18), (19) and (20)

$$\begin{aligned} &\begin{pmatrix} \mathbf{I}_1 & \mathbf{I}_0 \\ \mathbf{I}_0 & \mathbf{I}_0 \end{pmatrix}\begin{pmatrix} \hat{\mathbf{u}}(h) \\ \hat{\boldsymbol{\sigma}}'(h) \end{pmatrix} + \begin{pmatrix} \mathbf{I}_0 & \mathbf{I}_0 \\ \mathbf{I}_1 & \mathbf{I}_0 \end{pmatrix}\begin{pmatrix} \hat{\boldsymbol{\xi}}(h) \\ \hat{\boldsymbol{\sigma}}''(h) \end{pmatrix} \\ &\quad = \mathbf{J}\begin{pmatrix} \mathbf{I}_1 & \mathbf{I}_0 \\ \mathbf{I}_0 & \mathbf{I}_0 \end{pmatrix}\begin{pmatrix} \hat{\mathbf{u}}(0) \\ \hat{\boldsymbol{\sigma}}'(0) \end{pmatrix} + \mathbf{J}\begin{pmatrix} \mathbf{I}_0 & \mathbf{I}_0 \\ \mathbf{I}_1 & \mathbf{I}_0 \end{pmatrix}\begin{pmatrix} \hat{\boldsymbol{\xi}}(0) \\ \hat{\boldsymbol{\sigma}}''(0) \end{pmatrix}, \end{aligned} \tag{21}$$

$$\begin{aligned} &\begin{pmatrix} \mathbf{I}_0 & \mathbf{I}_1 \\ \mathbf{I}_0 & \mathbf{I}_0 \end{pmatrix}\begin{pmatrix} \hat{\mathbf{u}}(h) \\ \hat{\boldsymbol{\sigma}}'(h) \end{pmatrix} + \begin{pmatrix} \mathbf{I}_0 & \mathbf{I}_0 \\ \mathbf{I}_0 & \mathbf{I}_1 \end{pmatrix}\begin{pmatrix} \hat{\boldsymbol{\xi}}(h) \\ \hat{\boldsymbol{\sigma}}''(h) \end{pmatrix} \\ &\quad = \mathbf{K}\begin{pmatrix} \mathbf{I}_1 & \mathbf{I}_0 \\ \mathbf{I}_0 & \mathbf{I}_0 \end{pmatrix}\begin{pmatrix} \hat{\mathbf{u}}(0) \\ \hat{\boldsymbol{\sigma}}'(0) \end{pmatrix} + \mathbf{K}\begin{pmatrix} \mathbf{I}_0 & \mathbf{I}_0 \\ \mathbf{I}_1 & \mathbf{I}_0 \end{pmatrix}\begin{pmatrix} \hat{\boldsymbol{\xi}}(0) \\ \hat{\boldsymbol{\sigma}}''(0) \end{pmatrix}, \end{aligned} \tag{22}$$

$$\begin{aligned} &\mathbf{G}\begin{pmatrix} \mathbf{I}_0 & \mathbf{I}_1 \\ \mathbf{I}_0 & \mathbf{I}_0 \end{pmatrix}\begin{pmatrix} \hat{\mathbf{u}}(0) \\ \hat{\boldsymbol{\sigma}}'(0) \end{pmatrix} + \mathbf{G}\begin{pmatrix} \mathbf{I}_0 & \mathbf{I}_0 \\ \mathbf{I}_1 & \mathbf{I}_0 \end{pmatrix}\begin{pmatrix} \hat{\boldsymbol{\xi}}(0) \\ \hat{\boldsymbol{\sigma}}''(0) \end{pmatrix} \\ &\quad = \mathbf{H}\begin{pmatrix} \mathbf{I}_1 & \mathbf{I}_0 \\ \mathbf{I}_0 & \mathbf{I}_0 \end{pmatrix}\begin{pmatrix} \hat{\mathbf{u}}(0) \\ \hat{\boldsymbol{\sigma}}'(0) \end{pmatrix} + \mathbf{H}\begin{pmatrix} \mathbf{I}_0 & \mathbf{I}_0 \\ \mathbf{I}_1 & \mathbf{I}_0 \end{pmatrix}\begin{pmatrix} \hat{\boldsymbol{\xi}}(0) \\ \hat{\sigma}''(0) \end{pmatrix}. \end{aligned} \tag{23}$$

Here $\mathbf{I}_0$ and $\mathbf{I}_1$ are the null and identity matrices as defined in Eq. (13). Eqs. (21),(22) and (23) can be written as

$$\mathbf{I}_{11}\begin{pmatrix}\hat{\mathbf{u}}(h)\\ \hat{\boldsymbol{\sigma}}'(h)\end{pmatrix}+\mathbf{I}_{21}\begin{pmatrix}\hat{\boldsymbol{\xi}}(h)\\ \hat{\boldsymbol{\sigma}}''(h)\end{pmatrix}=\mathbf{J}\mathbf{I}_{11}\begin{pmatrix}\hat{\mathbf{u}}(0)\\ \hat{\boldsymbol{\sigma}}'(0)\end{pmatrix}+\mathbf{J}\mathbf{I}_{21}\begin{pmatrix}\hat{\boldsymbol{\xi}}(0)\\ \hat{\boldsymbol{\sigma}}''(0)\end{pmatrix}, \tag{24}$$

$$\mathbf{I}_{12}\begin{pmatrix}\hat{\mathbf{u}}(h)\\ \hat{\boldsymbol{\sigma}}'(h)\end{pmatrix}+\mathbf{I}_{22}\begin{pmatrix}\hat{\boldsymbol{\xi}}(h)\\ \hat{\boldsymbol{\sigma}}''(h)\end{pmatrix}=\mathbf{K}\mathbf{I}_{11}\begin{pmatrix}\hat{\mathbf{u}}(0)\\ \hat{\boldsymbol{\sigma}}'(0)\end{pmatrix}+\mathbf{K}\mathbf{I}_{21}\begin{pmatrix}\hat{\boldsymbol{\xi}}(0)\\ \hat{\boldsymbol{\sigma}}''(0)\end{pmatrix}, \tag{25}$$

$$\mathbf{G}\mathbf{I}_{12}\begin{pmatrix}\hat{\mathbf{u}}(0)\\ \hat{\boldsymbol{\sigma}}'(0)\end{pmatrix}+\mathbf{G}\mathbf{I}_{21}\begin{pmatrix}\hat{\boldsymbol{\xi}}(0)\\ \hat{\boldsymbol{\sigma}}''(0)\end{pmatrix}=\mathbf{H}\mathbf{I}_{11}\begin{pmatrix}\hat{\mathbf{u}}(0)\\ \hat{\boldsymbol{\sigma}}'(0)\end{pmatrix}+\mathbf{H}\mathbf{I}_{21}\begin{pmatrix}\hat{\boldsymbol{\xi}}(0)\\ \hat{\boldsymbol{\sigma}}''(0)\end{pmatrix}. \tag{26}$$

From Eq. (26), we have,

$$\begin{aligned}\begin{pmatrix}\hat{\boldsymbol{\xi}}(0)\\ \hat{\boldsymbol{\sigma}}''(0)\end{pmatrix}&=(\mathbf{G}\mathbf{I}_{21}-\mathbf{H}\mathbf{I}_{21})^{-1}(\mathbf{H}\mathbf{I}_{11}\\ &\quad-\mathbf{G}\mathbf{I}_{12})\begin{pmatrix}\hat{\mathbf{u}}(0)\\ \hat{\boldsymbol{\sigma}}'(0)\end{pmatrix}\\ &=\mathbf{L}\begin{pmatrix}\hat{\mathbf{u}}(0)\\ \hat{\boldsymbol{\sigma}}'(0)\end{pmatrix}.\end{aligned} \tag{27}$$

Substitution of Eq. (27) into Eqs. (24) and (25) yields

$$\begin{pmatrix}\mathbf{I}_{11} & \mathbf{I}_{21}\\ \mathbf{I}_{12} & \mathbf{I}_{22}\end{pmatrix}\begin{pmatrix}\begin{pmatrix}\hat{\mathbf{u}}(h)\\ \hat{\boldsymbol{\sigma}}'(h)\end{pmatrix}\\ \begin{pmatrix}\hat{\boldsymbol{\xi}}(h)\\ \hat{\boldsymbol{\sigma}}''(h)\end{pmatrix}\end{pmatrix}=\begin{pmatrix}\mathbf{J}\mathbf{I}_{11}+\mathbf{J}\mathbf{I}_{21}\mathbf{L}\\ \mathbf{K}\mathbf{I}_{11}+\mathbf{K}\mathbf{I}_{21}\mathbf{L}\end{pmatrix}\begin{pmatrix}\hat{\mathbf{u}}(0)\\ \hat{\boldsymbol{\sigma}}'(0)\end{pmatrix}. \tag{28}$$

From Eq. (28), we have

$$\begin{pmatrix} \begin{pmatrix} \hat{\mathbf{u}}(h) \\ \hat{\boldsymbol{\sigma}}'(h) \end{pmatrix} \\ \begin{pmatrix} \hat{\boldsymbol{\xi}}(h) \\ \hat{\boldsymbol{\sigma}}''(h) \end{pmatrix} \end{pmatrix} = \begin{pmatrix} \mathbf{I}_{11} & \mathbf{I}_{21} \\ \mathbf{I}_{12} & \mathbf{I}_{22} \end{pmatrix}^{-1} \begin{pmatrix} \mathbf{J}\mathbf{I}_{11} + \mathbf{J}\mathbf{I}_{21}\mathbf{L} \\ \mathbf{K}\mathbf{I}_{11} + \mathbf{K}\mathbf{I}_{21}\mathbf{L} \end{pmatrix} \begin{pmatrix} \hat{\mathbf{u}}(0) \\ \hat{\boldsymbol{\sigma}}'(0) \end{pmatrix}$$

$$= \mathbf{F} \begin{pmatrix} \hat{\mathbf{u}}(0) \\ \hat{\boldsymbol{\sigma}}'(0) \end{pmatrix}. \tag{29}$$

Here $\mathbf{F} = (\mathbf{F}_1, \mathbf{F}_2)^T$ is a general transfer matrix that relates the variables on the panel top surface $z = h$ to the displacements and z-component stresses on the bottom surface. From Eq. (29), we have

$$\begin{pmatrix} \hat{\mathbf{u}}(h) \\ \hat{\boldsymbol{\sigma}}'(h) \end{pmatrix} = \mathbf{F}_1 \begin{pmatrix} \hat{\mathbf{u}}(0) \\ \hat{\boldsymbol{\sigma}}'(0) \end{pmatrix} = \mathbf{T} \begin{pmatrix} \hat{\mathbf{u}}(0) \\ \hat{\boldsymbol{\sigma}}'(0) \end{pmatrix}. \tag{30}$$

Here $\mathbf{T} = \mathbf{F}_1$ is a special transfer matrix that links together the displacements and z-component stresses on the top and bottom surfaces. Eq. (30) is also applicable for multi-layer panels. In that case, $\mathbf{T}$ is a grand transfer matrix that is the chain multiplication of all the layer-wise transfer matrices. For instance, for a three-layer sandwich panel, the grand transfer matrix is

$$\mathbf{T}=\mathbf{T}^{(3)}\mathbf{T}^{(2)}\mathbf{T}^{(1)}. \tag{31}$$

Here $\mathbf{T}^{(3)}$, $\mathbf{T}^{(2)}$, and $\mathbf{T}^{(1)}$ are the transfer matrices for the top face layer, middle core layer, and bottom face layer, respectively. In obtaining Eq. (31), we used the fact that the displacements and the z-component stresses must be continuous at the layer interfaces. In the state space method [21], the displacements and the z-component stresses are the state variables for each layer. Eq. (30) can also be written out explicitly as

$$\begin{pmatrix} \hat{u}^{(top)} \\ \hat{v}^{(top)} \\ \hat{w}^{(top)} \\ \hat{\sigma}_{zx}^{(top)} \\ \hat{\sigma}_{zy}^{(top)} \\ \hat{\sigma}_{zz}^{(top)} \end{pmatrix} = \begin{pmatrix} t_{11} & t_{12} & t_{13} & t_{14} & t_{15} & t_{16} \\ t_{21} & t_{22} & t_{23} & t_{24} & t_{25} & t_{26} \\ t_{31} & t_{32} & t_{33} & t_{34} & t_{35} & t_{36} \\ t_{41} & t_{42} & t_{43} & t_{44} & t_{45} & t_{46} \\ t_{51} & t_{52} & t_{53} & t_{54} & t_{55} & t_{56} \\ t_{61} & t_{62} & t_{63} & t_{64} & t_{65} & t_{66} \end{pmatrix} \begin{pmatrix} \hat{u}^{(bot)} \\ \hat{v}^{(bot)} \\ \hat{w}^{(bot)} \\ \hat{\sigma}_{zx}^{(bot)} \\ \hat{\sigma}_{zy}^{(bot)} \\ \hat{\sigma}_{zz}^{(bot)} \end{pmatrix}. \quad (32)$$

Here the superscript *Top* stands for the top panel surface, and the superscript *Bot*stands for the bottom panel surface. Eq. (32) provides the key for solving the problem of acoustic transmission, which is the focus of the present study.

2.4 Acoustic transmission

We turn now to the determination of the sound transmission through the structural panel as depicted in Fig. 1. The incident acoustic wave can be written as

$$p(x,y,z,t)=Ae^{ik_{0x}x+ik_{0y}y+ik_{0z}z}e^{-i\omega t}. \quad (33)$$

Here, A is the amplitude of the incident pressure wave, $k_0 = \omega/c$ is the wave number in the air, and

$$\begin{aligned} k_{0x} &= k_0 \sin\theta\cos\phi \\ k_{0y} &= k_0 \sin\theta\sin\phi \\ k_{0z} &= k_0 \cos\theta \end{aligned} \quad (34)$$

Here, θ and ϕ are the polar and azimuthal angles. Without the loss of generality, we assume $\phi = 0$ in this study. Due to the excitation of the incident wave, the panel will undergo structural vibration. Suppose the displacements on the top and bottom surfaces can be expressed as

$$w^{(top)} = Te^{ik_{px}x+ik_{py}y}e^{-i\omega t}$$
$$w^{(bot)} = Be^{ik_{px}x+ik_{py}y}e^{-i\omega t} \quad (35)$$

Here, the values of T and B are to be determined as shown below. To ensure contact continuity at the panel-air interface, we must have [15], [16], [17], [18], [19] and [20],

$$k_{px} = k_{0x}$$
$$k_{py} = k_{0y} \quad (36)$$

The total pressure on the top and bottom panel surfaces can be written as

$$p^{(top)} = -\frac{\rho_0(-i\omega)^2}{ik_z}Te^{ik_{px}x+ik_{py}y}e^{-i\omega t}$$
$$p^{(bot)} = -\frac{\rho_0(-i\omega)^2}{-ik_z}Be^{ik_{px}x+ik_{py}y}e^{-i\omega t} + 2Ae^{ik_{0x}x+ik_{0y}y}e^{-i\omega t} \quad (37)$$

Here 2A is the amplitude of the blocked pressure, and

$$k_z = \sqrt{k_0^2 - \left(k_{px}^2 + k_{py}^2\right)}. \quad (38)$$

Combining Eqs. (34), (36) and (38), we see that

$k_z = k_0\cos\theta$. (39)

From Eq. (35), we get,

$$\hat{w}^{(top)} = T$$
$$\hat{w}^{(bot)} = B \quad (40)$$

From Eq. (37), we get

$$\hat{\sigma}_{zz}^{(top)} = -p^{(top)} = \frac{\rho_0(-\mathrm{i}\omega)^2}{\mathrm{i}k_z} T$$
$$\hat{\sigma}_{zz}^{(bot)} = -p^{(bot)} = \frac{\rho_0(-\mathrm{i}\omega)^2}{-\mathrm{i}k_z} B - 2A \tag{41}$$

Also note that the shear stresses on the top and bottom panel surfaces must vanish

$$\hat{\sigma}_{zx}^{(top)} = \hat{\sigma}_{zy}^{(top)} = 0$$
$$\hat{\sigma}_{zx}^{(bot)} = \hat{\sigma}_{zy}^{(bot)} = 0 \tag{42}$$

Substitution of Eqs. (40), (41) and (42) into Eq. (32) yields

$$\begin{pmatrix} \hat{u}^{(top)} \\ \hat{v}^{(top)} \\ T \\ 0 \\ 0 \\ \frac{\rho_0(-\mathrm{i}\omega)^2}{\mathrm{i}k_z} T \end{pmatrix} = \begin{pmatrix} t_{11} & t_{12} & t_{13} & t_{14} & t_{15} & t_{16} \\ t_{21} & t_{22} & t_{23} & t_{24} & t_{25} & t_{26} \\ t_{31} & t_{32} & t_{33} & t_{34} & t_{35} & t_{36} \\ t_{41} & t_{42} & t_{43} & t_{44} & t_{45} & t_{46} \\ t_{51} & t_{52} & t_{53} & t_{54} & t_{55} & t_{56} \\ t_{61} & t_{62} & t_{63} & t_{64} & t_{65} & t_{66} \end{pmatrix} \begin{pmatrix} \hat{u}^{(bot)} \\ \hat{v}^{(bot)} \\ B \\ 0 \\ 0 \\ \frac{\rho_0(-\mathrm{i}\omega)^2}{-\mathrm{i}k_z} B - 2A \end{pmatrix}. \tag{43}$$

From Eq. (43), it is straightforward to solve for the six unknowns, including B and T. From there, the acoustic transmission coefficient τ and reflection coefficient r can be calculated. The results are given below

$$\tau = \left| \frac{-2NR\kappa}{-M_1\kappa^2 + (M_2 + M_3)\mathrm{i}R\kappa + M_4R^2} \right|^2, \tag{44}$$

$$r = \left| \frac{-M_1\kappa^2 + (M_2 - M_3)\mathrm{i}R\kappa - M_4R^2}{-M_1\kappa^2 + (M_2 + M_3)\mathrm{i}R\kappa + M_4R^2} \right|^2. \tag{45}$$

Here, the parameters R and κ are defined as

$$R = \rho_0 c_0 \omega$$
$$\kappa = Re(k_z/k_0) = \cos\theta \tag{46}$$

Other parameters in Eqs. (44) and (45) are defined as

$$N = \det \begin{pmatrix} 1 & 0 & t_{11} & t_{12} & t_{13} & t_{16} \\ 0 & 1 & t_{21} & t_{22} & t_{23} & t_{26} \\ 0 & 0 & t_{31} & t_{32} & t_{33} & t_{36} \\ 0 & 0 & t_{41} & t_{42} & t_{43} & t_{46} \\ 0 & 0 & t_{51} & t_{52} & t_{53} & t_{56} \\ 0 & 0 & t_{61} & t_{62} & t_{63} & t_{66} \end{pmatrix}, \tag{47}$$

$$M_1 = \det \begin{pmatrix} 1 & 0 & t_{11} & t_{12} & t_{13} \\ 0 & 1 & t_{21} & t_{22} & t_{23} \\ 0 & 0 & t_{41} & t_{42} & t_{43} \\ 0 & 0 & t_{51} & t_{52} & t_{53} \\ 0 & 0 & t_{61} & t_{62} & t_{63} \end{pmatrix},$$
$$M_2 = \det \begin{pmatrix} 1 & 0 & t_{11} & t_{12} & t_{13} \\ 0 & 1 & t_{21} & t_{22} & t_{23} \\ 0 & 0 & t_{31} & t_{32} & t_{33} \\ 0 & 0 & t_{41} & t_{42} & t_{43} \\ 0 & 0 & t_{51} & t_{52} & t_{53} \end{pmatrix}, \tag{48}$$

$$M_3 = \det \begin{pmatrix} 1 & 0 & t_{11} & t_{12} & t_{16} \\ 0 & 1 & t_{21} & t_{22} & t_{26} \\ 0 & 0 & t_{41} & t_{42} & t_{46} \\ 0 & 0 & t_{51} & t_{52} & t_{56} \\ 0 & 0 & t_{61} & t_{62} & t_{66} \end{pmatrix},$$

$$M_4 = \det \begin{pmatrix} 1 & 0 & t_{11} & t_{12} & t_{16} \\ 0 & 1 & t_{21} & t_{22} & t_{26} \\ 0 & 0 & t_{31} & t_{32} & t_{36} \\ 0 & 0 & t_{41} & t_{42} & t_{46} \\ 0 & 0 & t_{51} & t_{52} & t_{56} \end{pmatrix}. \tag{49}$$

Here *det* stands for the determination of a matrix. Substitution of (46) into (44) and (45)yields

$$\tau = \left| \frac{-2N\rho_0 c_0 \omega \cos\theta}{-M_1 \cos^2\theta + (M_2 + M_3) i\rho_0 c_0 \omega \cos\theta + M_4 (\rho_0 c_0 \omega)^2} \right|^2, \tag{50}$$

$$r = \left| \frac{-M_1 \cos^2\theta + (M_2 - M_3) i\rho_0 c_0 \omega \cos\theta - M_4 (\rho_0 c_0 \omega)^2}{-M_1 \cos^2\theta + (M_2 + M_3) i\rho_0 c_0 \omega \cos\theta + M_4 (\rho_0 c_0 \omega)^2} \right|^2. \tag{51}$$

Eqs. (50) and (51) are the central results of this study. They represent the exact analytical solutions of the acoustic transmission and reflection coefficients for general anisotropic layered structures. To our knowledge, such explicit and concise expressions for these two coefficients under such general conditions have not yet been reported. These analytical expressions clearly show the dependence of the acoustic transmission and reflection coefficients on the source frequency, incident angle, and other material properties. For instance, Eqs. (50) and (51) reveal that a full acoustic reflection occurs at the incident angle of θ = 90°. This is expected because the incident acoustic wave is traveling parallel to the panel surface. Therefore no acoustic energy is transmitted through the panel, i.e., $\tau = 0$.

The effect of material properties is incorporated in the values of N, and M_1 through M_4 as defined in Eqs. (47),(48) and (49).

With the acoustic transmission coefficient determined, the sound transmission loss (TL) is defined as

$$\mathrm{TL} = 10\log_{10}\left(\frac{1}{\tau}\right). \tag{52}$$

For a diffuse sound field, the angle-averaged transmission coefficient is used to compute TL,

$$\bar{\tau} = \frac{\int_0^{2\pi}\left[\int_0^{\pi/2}\tau(\theta,\phi)\sin\theta\cos\theta\mathrm{d}\theta\right]\mathrm{d}\phi}{\int_0^{2\pi}\left[\int_0^{\pi/2}\sin\theta\cos\theta\mathrm{d}\theta\right]\mathrm{d}\phi}. \tag{53}$$

Having derived the analytical solution for the sound transmission coefficient, we next present numerical examples. In our calculations, we take the air density to beρ_0 = 1.25 kg/m^3, and the speed of sound in the air to be c_0 = 340 m/s.

3. Results

3.1 Single-layer panel

The first example is taken from the work by Leppington and his colleagues [7], who considered the sound transmission for an aluminum panel of thickness h = 2.5 mm. In this example, the properties of aluminum included density (ρ = 2700 kg/m^3), Young's modulus (E = 71 GPa), Poisson's ratio (μ = 0.33), and loss factor (η = 0).

Fig. 2 shows a plot of the transmission coefficient τ as a function of the incident angle θ and the frequency *f*. Note that for a given frequency, there is one transmission peak in the plot that occurs near the grazing angle θ = 90°. For a given frequency greater than the critical frequency (in this case, *fc* = 4800 Hz), there is a second transmission peak τ = 1 at a moderate incident angle This second peak is a phenomenon of acoustic coincidence that is caused by the matching of the wave number of the bending wave in the panel with the trace wave number in the ambient air [9] and [11]. Above the critical frequency, the coincident transmission dominates, while the near-grazing transmission decreases.

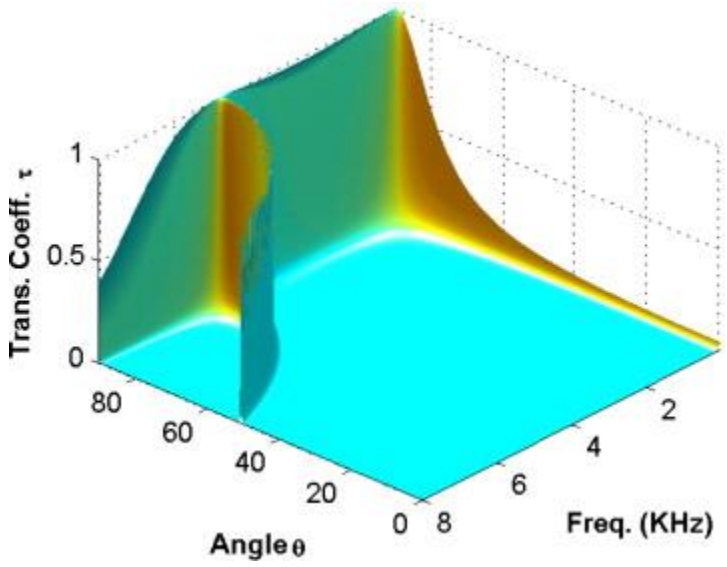

Fig. 2. *Plot of the transmission coefficients τ as a function of the incident angle θ and the frequency f for a single layer aluminum panel.*

When the incident acoustic wave arises from a diffuse sound field such as an echoic room, then the measured transmission coefficient is generally an averaged value, as defined in Eq. (53). Fig. 3 shows a comparison between the transmission loss values generated from model-based predictions with those measured experimentally. The experimental data was obtained from an aluminum panel of finite dimensions 1.4 m × 0.9 m [7]. The finite dimensions and boundary constraints of the panel

caused acoustic resonances or eigen-vibrations in the in-plane directions. These resonanances are manifest in the experimental curve as fine-scale oscillations (modal resonance peaks and dips). In contrast, the modeling curve is smooth and void of fine-scale oscillations because the modeled panel was assumed to be infinite in the in-plane directions. The effect of panel size is not the prime concern here, although some researchers have analyzed this issue specifically [22] and [23].

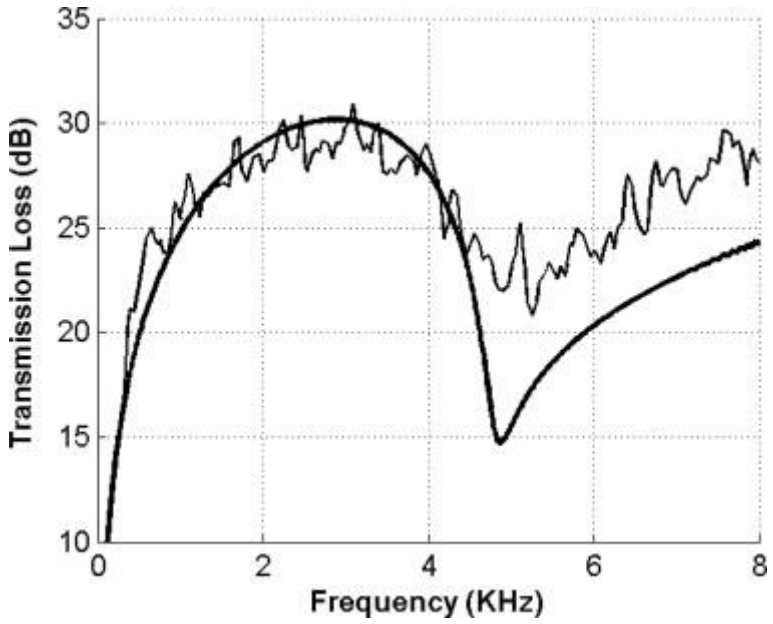

Fig. 3. *A comparison of sound transmission loss for the aluminum panel example: prediction from the 3-D elasticity theory (thick line), and data from experimental measurement (thin line).*

The comparison shown in Fig. 3 reveals that the model accurately predicts the critical coincident frequency at ~4800 Hz. In addition, the agreement between the model prediction and the measured data is excellent for frequencies less than the coincident frequency. For frequencies greater than the coincident frequency, a deviation of about 5 dB is noted between theory and experiment. This discrepancy is attributed to acoustic damping of the material, which plays a more important role above the critical coincident frequency [24]. However, in our modeling we assumed no damping, i.e., zero loss factorη = 0 for the aluminum panel.

3.2 Sandwich panel

Our second example is taken from Moore and Lyon [8], who considered a sandwich panel with two 6.35 mm (1/4-in) plywood face sheets and a 76.2 mm (3-in) styrofoam core. For modeling purposes, we assume that the plywood layer and the core layer are both isotropic materials. The property values used for the core include density (ρ = 16 kg/m^3), Young's modulus (E = 12.5 MPa), and shear modulus (G = 3.1 MPa). For the plywood face sheet, the Young's modulus is E = 7 GPa, area density of the face layer$m$ = 3.73 kg/m^3, and Poisson ratio μ = 0.38. The calculated and measured transmission loss values are depicted in Fig. 4. Because this is a three-layer compound panel, the grand transfer matrix as defined in Eq. (31) was used to obtain the predicted values from the 3-D elasticity method.

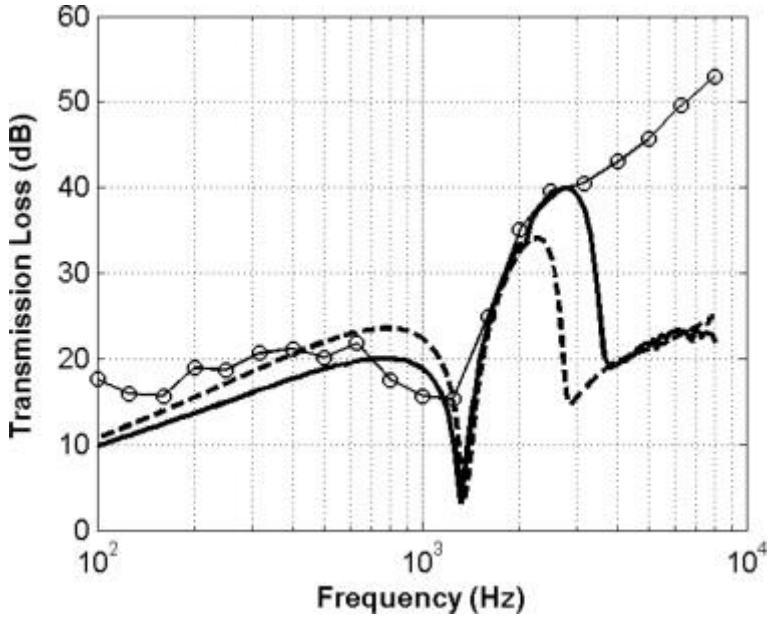

Fig. 4. *A comparison of sound transmission loss for the sandwich panel example: prediction from the 3-D elasticity theory (thick line), prediction from the Moore–Lyon method (thick dashed line), and data from experimental measurement (thin line with circles).*

Please cite this article as: Changzheng Huang, Steven Nutt, **Sound transmission prediction by 3-D elasticity theory**, Applied Acoustics, Volume 70, Issue 5, May 2009, Pages 730-736, ISSN 0003-682X, http://dx.doi.org/10.1016/j.apacoust.2008.09.003.

For comparison purposes, the transmission loss calculated from the Moore–Lyon method [8] is also displayed in Fig. 4. In the Moore–Lyon method, an approximate displacement field is assumed for all the sandwich layers, and the virtual work principle is applied to determine the unknown coefficients in the assumed displacement expressions. This is a typical approach used in approximate methods. Also shown in Fig. 4 is the measured transmission loss. The panel used in the experimental measurement was 1.22 m × 2.44 m (4 feet by 8 feet). The panel size and the boundary mounting conditions are the main differences between the model calculations and the experiment.

Despite these differences, the model-based predictions closely match the measured data up to a frequency of 3 kHz. The predicted coincident frequency as indicated by the first large dip in the modeling curves is nearly identical to the measured coincident frequency. At frequencies greater than 3 kHz, the calculated predictions from both modeling methods deviate substantially from the measured data, although the difference is approximately constant. In the high frequency range, material damping is an important factor affecting the sound transmission loss. This effect has not been included in the model, where a loss factor value of $\eta = 0$ was used in all calculations.

Note that although the Moore–Lyon method and the 3-D elasticity method predicted nearly identical values of coincident frequency, they also yielded noticeable differences in transmission loss values in frequency ranges above and below the coincident frequency. Since the numerical results from the 3-D elasticity method are computed from the exact solution to the 3-D elasticity equations, it is expected that the predicted transmission loss from the 3-D elasticity method is more accurate than other modeling methods. Therefore the differences between the 3-D elasticity predictions and the Moore–Lyon predictions indicate how much the assumed displacement field in the Moore–Lyon method differed from the actual displacement field.

Please cite this article as: Changzheng Huang, Steven Nutt, **Sound transmission prediction by 3-D elasticity theory**, Applied Acoustics, Volume 70, Issue 5, May 2009, Pages 730-736, ISSN 0003-682X, http://dx.doi.org/10.1016/j.apacoust.2008.09.003.

4. Discussions

The 3-D formulation and solution for sound transmission and reflection can be compared to the conventional 2-D (beam) formulation and other special cases to highlight the differences. Note that the 3-D elasticity model applies only to multi-layered panels infinite in the in-plane (*x*-, *y*)-directions. This is a basic assumption used in Eq. (8). If the in-plane dimensions were not infinite, then Eq. (8) would not be valid, and might take different forms. For instance, for a finite rectangular panel, Eq. (8) would have become a double integration over the wave number space

$$\mathbf{u}(x,y,z,t) = \mathrm{e}^{-\mathrm{i}\omega t}\int_{k_x}\int_{k_y}\hat{\mathbf{u}}(k_x,k_y,z)\mathrm{e}^{\mathrm{i}k_x x}\mathrm{e}^{\mathrm{i}k_y y}\mathrm{d}k_x\mathrm{d}k_y$$
$$\boldsymbol{\sigma}(x,y,z,t) = \mathrm{e}^{-\mathrm{i}\omega t}\int_{k_x}\int_{k_y}\hat{\boldsymbol{\sigma}}(k_x,k_y,z)\mathrm{e}^{\mathrm{i}k_x x}\mathrm{e}^{\mathrm{i}k_y y}\mathrm{d}k_x\mathrm{d}k_y \qquad (54)$$

We did not deal with the case of finite panel size in this study. For general boundary conditions, the analytical expressions for the spectral variables in Eq. (54) are often too involved to permit an analytical derivation. Under these circumstances, a numerical method would be more suitable.

In practical applications, panel structures often have in-plane dimensions that are significantly larger (by orders of magnitude) than the panel thickness. Under such conditions, the 3-D elasticity model is a good approximation, as demonstrated by the panel examples presented earlier.

For the case of a 2-D structure such as a sandwich beam, the 3-D elasticity model can be simplified accordingly. For plane stress or plane strain problems, some components of the displacement or stresses will not vary in one of the in-plane directions, say in the *y*-direction. In this case, the governing Eqs. (8), (9) and (10) can be simplified by setting$ky = 0$, and Eq. (10) would become

$$\mathbf{B}_2 = \mathbf{D}_3\mathbf{C}\mathbf{D}_3^{\mathrm{T}}$$
$$\mathbf{B}_1 = (\mathrm{i}k_x)\mathbf{D}_1\mathbf{C}\mathbf{D}_3^{\mathrm{T}} + (\mathrm{i}k_x)\mathbf{D}_3\mathbf{C}\mathbf{D}_1^{\mathrm{T}}$$
$$\mathbf{B}_0 = (\mathrm{i}k_x)(\mathrm{i}k_x)\mathbf{D}_1\mathbf{C}\mathbf{D}_1^{\mathrm{T}} \tag{55}$$

Eq. (55) can be further reduced by employing the plane stress or plane strain conditions. Note that the final expression for sound transmission obtained from Eq. (55) is an exact analytical solution. This can be considered as the 2-D counterpart for the 3-D elasticity model.

Numerical approaches often start with an assumption of the displacement field in the panel thickness direction [8] and [9]. For instance, the displacement distribution in the out-of-plane direction may be approximated by a third-order polynomial. Such a numerical approximation is, of course, a special case of the 3-D elasticity formulation. This can be obtained from Eq. (14) by truncating the expansion series of the exponential factor to the third-order

$$\begin{pmatrix} \hat{\mathbf{u}}(z) \\ \hat{\boldsymbol{\xi}}(z) \end{pmatrix} = \mathrm{e}^{\mathbf{A}z}\begin{pmatrix} \hat{\mathbf{u}}(0) \\ \hat{\boldsymbol{\xi}}(0) \end{pmatrix}$$
$$\approx \left[\mathbf{I} + \mathbf{A}z + \frac{1}{2!}(\mathbf{A}z)^2 + \frac{1}{3!}(\mathbf{A}z)^3\right]\begin{pmatrix} \hat{\mathbf{u}}(0) \\ \hat{\boldsymbol{\xi}}(0) \end{pmatrix}. \tag{56}$$

The accuracy of a numerical approximation depends on the higher-order terms that have been truncated out. For thin panels, the approximation in Eq. (56) provides accuracy that is usually sufficient, but for thick panels, a third-order approximation may not be adequate. For the analytical solution, fortunately, one does not need to worry about this effect, as it has been taken care of automatically in the matrix exponential term in Eq.(14), whether it is a thin panel or a thick panel. This is one of the advantages of the analytical 3-D elasticity model. The Moore–Lyon modeling approach in the sandwich panel example is an approximate method in which a displacement field is

assumed for all panel layers. The comparison between the Moore–Lyon method and the 3-D elasticity model is illustrated in Fig. 4.

5. Conclusions

The 3-D elasticity equations and a general anisotropic stress–strain relationship were used to derive an analytical solution for the prediction of sound transmission through panels in an exact manner. The analytical solution was used to predict sound transmission through specific structural panels, including a single-layer panel and a sandwich panel. The accuracy of the model prediction of sound transmission loss was supported by agreement with experimental data. This was particularly true for the prediction of panel coincident frequency, as well as for the prediction of transmission loss at low frequencies. Discrepancies at higher frequencies arose because of material damping, which was not accounted for in the model. The effect of material damping and panel size will be considered in future work.

Acknowledgements: The authors are grateful for financial support from the Merwyn C. Gill Foundation.

References:

1. Kurtze G, Watters BG. New wall design for high transmission loss or high damping. J Acoust Soc Am 1959;31:739–48.
2. Smolenski CP, Krokosky EM. Dilational-mode sound transmission in sandwich panels. J Acoust Soc Am 1973;54:1449–57.
3. Ramakrishnan JV, Koval LR. A finite element model for sound transmission through laminated composite plates. J Sound Vib 1987;112:433–46.
4. Ford RD, Lord P, Walker AW. Sound transmission through sandwich constructions. J Sound Vib 1967;5:9–21.
5. Narayanan S, Shanbhag RL. Sound transmission through a damped sandwich panel. J Sound Vib 1982;80:315–27.
6. Dym CL, Lang DC. Transmission loss of damped asymmetric sandwich panels with orthotropic cores. J Sound Vib 1983;88:299–319.

7. Leppington FG, Heron KH, Broadbent EG, Mead SM. Resonant and nonresonant acoustic properties of elastic panels. II. The transmission problem. Proc Royal Soc London 1987;A412:309–37.
8. Moore JA, Lyon RH. Sound transmission loss characteristics of sandwich panel constructions. J Acoust Soc Am 1991;89:777–91.
9. Wang T, Sokolinsky VS, Rajaram S, Nutt SR. Assessment of sandwich models for the prediction of sound transmission loss in unidirectional sandwich panels. Appl Acoust 2005;66:245–62.
10. Sewell EC. Transmission of reverberant sound through a single-leaf partition surrounded by an infinite rigid baffle. J Sound Vib 1970;12:21–32.
11. Wang J, Lu TJ, Woodhouse J, Langley RS, Evans J. Sound transmission through lightweight double-leaf partitions: theoretical modeling. J Sound Vib 2005;286:817–47.
12. Guyader JL, Lesueur C. Acoustic transmission through orthotropic multilayered plates, part II: transmission loss. J Sound Vib 1978;58:69–86.
13. Liang C, Rogers CA, Fuller CR. Acoustic transmission and radiation analysis of adaptive shape memory alloy reinforced laminated plates. J Sound Vib 1991;145:23–41.
14. Munjal ML. Response of a multi-layered infinite plate to an oblique plane wave by means of transfer matrices. J Sound Vib 1993;162:333–43.
15. Kuo YM, Lin HJ, Wang CN. Sound transmission across orthotropic laminates with a 3D model. Appl Acoust 2007;69:951–9.
16. Lin HJ, Wang CN, Kuo YM. Sound transmission loss across specially orthotropic laminates. Appl Acoust 2007;68:1177–91.
17. Liu GR, Lam KY. Sound reflection and transmission of compliant plate-like structures by a plane sound wave excitation. J Sound Vib 2000;230:809–24.
18. Cai C, Liu GR, Lam KY. An exact method for analyzing sound reflection and transmission by anisotropic laminates submerged in fluids. Appl Acoust 2000;61:95–109.
19. Liu GR, Xi ZC. Elastic waves in anisotropic laminates. New York: CRC Press; 2002.
20. Skelton EA, James JH. Acoustics of anisotropic planar layered media. J Sound Vib 1992;152:157–74.
21. Ye JQ. Laminated composite plates and shells. London: Springer; 2003.
22. Villot M, Guigou C, Gagliardini L. Predicting the acoustical radiation of finite size multi-layered structures by applying spatial windowing on infinite structures. J Sound Vib 2001;245:433–55.
23. Lee JH, Ih JG. Significance of resonant sound transmission in finite single partitions. J Sound Vib 2004;277:881–93.
24. Fahy F, Gardonio P. Sound and structural vibration. New York: Elsevier; 2007.

Please cite this article as: Changzheng Huang, Steven Nutt, **Sound transmission prediction by 3-D elasticity theory**, Applied Acoustics, Volume 70, Issue 5, May 2009, Pages 730-736, ISSN 0003-682X, http://dx.doi.org/10.1016/j.apacoust.2008.09.003.